Nonsingular Fast Terminal Sliding Mode Based Model-Free Control: Application to Glycemia Regulation Systems

Y. Tian, H.P. Wang, Q. Wu, M.T. Hu

LaFCAS, School of Automation, Nanjing University of Science and Technology, 210094 Nanjing, China

N. Christov

LaFCAS and CRIStAL, University of Lille, 59655 Villeneuve d'Ascq, France

Corresponding author: hp.wang@njust.edu.cn

A new Model-Free Control (MFC) is derived to enhance the control performance of the well-known Nonlinear Integral Backstepping based MFC (NIB-MFC). A Nonsingular Fast Terminal Sliding Mode (NFTSM) component is added to NIB-MFC, which makes possible to compensate the estimation error of the time-delay estimation module of NIB-MFC. The obtained in this way new control structure is called NFTSM-MFC. The system stability with NFTSM-MFC is proved and the application of NFTSM-MFC for glycemia regulation is considered. The performances of NFTSM-MFC are compared with those of the NIB-MFC and the intelligent proportional control for a glucose-insulin model of type 1 diabetes patients under a long term simulation.

KEYWORDS: MFC, NFTSM-MFC, time-delay estimation, glycemia regulation.

1. Introduction

Model-based classical control methods are normally implemented on the condition that the system dynamics and operational circumstances are well known. However, for complex physical, socio-economic, or biological systems, where the system models are partially or completely unknown, these techniques give unsatisfactory results. It is a motivation for development of control procedures

that requires no model for the underlying system.

The data-driven control is such a control procedure which uses only the measurements from input and output, thus the unmodeled time varying uncertainties are not required known. The data driven concept was proposed firstly in the field of computer science, and has been introduced gradually into the control field. For instance, this concept has application in the control area of fault diagnosis and tolerance [40, 41]. Data-driven control methods have been developed into many types, which include virtual reference feedback tuning [6], iterative learning control [21], dynamic programming approach [45], neural network method [19], model free control [1, 13] and others [22, 33].

The data-driven based model-free control (MFC) consists of several branches, such as the algebraic estimation technique based MFC [1, 3, 13], the time-delay estimation based MFC [42], the learning adaptive based MFC [17], and the recursive MFC [35-37].

In this paper, MFC theory [1, 3, 13, 38, 44] and iPID control [2, 12] are adopted to design a controller which uses an ultra-local model for small time window to approximate the system dynamics. The unmodeled system dynamics in the ultra-local model are included in a function F which an algebraic estimator is used to estimate and update [1, 3, 13]. Thus the order of the model can be reduced to fit system dynamics while the system can be efficiently controlled by a simple law, such as the intelligent proportional iP controller [1, 3, 13]. To avoid the difficulties in implementing the algebraic estimation, time-delay estimation (TDE) can be used instead [42, 44]. To improve control performances, the model-free control can be combined with a nonlinear integral backstepping control, obtaining thus the so-called Nonlinear Integral Backstepping based MFC (NIB-MFC) [38].

In current paper, a relative new model-free control structure called NFTSM-MFC is proposed. The proposed model-free control is obtained by adding a NFTSM component to the NIB-MFC structure which makes it possible to compensate the estimation error in TDE.

Artificial pancreas, combining insulin injection with advanced intelligent equipment to describe the functioning of a healthy pancreas, is the most potential solution for T1DM. Various control strategies for ar-

tificial pancreas are designed: classical model-based techniques [10, 20, 32], model based predictive controller [5, 8, 9, 30, 31], and model independent based control, such as PID [7, 26, 29] and data-driven based model-free control [4, 14, 27, 46].

A precise physiological model which describes corresponding physiological characteristics adequately is hard to obtain. The limitations of the existing blood glucose models make it difficult to use model based control algorithms which take a long time in trials. As for non-model based controllers, such as PID controllers, it is also hard to overcome disturbances and uncertainties. By comparison, the glycemia regulation can be efficiently done by model-free controllers, and have the advantage of easy tuning and implementation.

The structure of the paper is introduced in this paragraph. In Section 2, the ultra-local model and corresponding TDE based iP control (TDE-iPC) are briefly introduced. In Section 3, NFTSM-MFC is proposed, and its system stability is analyzed. Then a glucose-insulin dynamics model of T1DM for a long-term simulation is presented in Section 4. In Section 5, the TDE-iPC, NIB-MFC and NFTSM-MFC are applied to this model and their performances are compared for the parameter values of three virtual patients. Finally, Section 6 gives some conclusions comments.

2. iP Control Using Time-Delay Estimation Technics

In this section, a new iP controller using TDE instead of algebraic estimation is proposed.

2.1. Ultra-local Model and iP Controller

A general SISO unknown system could be described by the ultra-local model [1, 2, 12, 14]:

$$y^{(\nu)} = F + \alpha u, \tag{1}$$

where y denotes the system output, $y^{(\nu)}$ is the derivative of y with order $\nu \geq 1$, andnd u denotes the system input. The parameter $\alpha \in \Re$ is chosen to guarantee that αu and $y^{(\nu)}$ are in the same quantitative level. F denotes the disturbances and system dynamics which are hard to model. The above referred integer

v is usually chosen to 1 or 2. In turn, F can be obtained through the measurements of u and y, which can be continuously updated.

For the system (1) with $v = 1$, the following iP controller is proposed in [1]:

$$u = -\frac{\widehat{F} - \dot{y}_d - K_p e}{\alpha}, \tag{2}$$

where $\dot{y}_d$ represents the desired reference y_d derivative, $e = y_d - y$ denotes their corresponding tracking trajectory error, K_p is the proportional parameter and $\widehat{F}$ is an actual estimate of F. From (1-2), one obtains the closed-loop system equation

$$\dot{e} + K_p e + e_{est} = 0, \tag{3}$$

where $e_{est} = F - \widehat{F}$ is the error of estimation of F. If $e_{est} = e$ in (3), the tuning of the gain K_p is relatively easy.

2.2. TDE Based iP Controller

The crucial point of the iP control and of MFC in general, is the estimation of F. In this part, the TDE method is adopted. This TDE method estimates the lumped disturbances and unmodeled dynamics with time-delayed information. The selected Time-delay which is denoted as L should be small enough to keep functioning and usually chosen to be the same time value as the sampling time of the embedded systems, noting that the sampling time usually meets the requirements to system dynamics. The referred TDE can be illustrated as follows

$$\widehat{F}(t) \approx F(t - L) = \dot{y}(t - L) - \alpha u(t - L) \tag{4}$$
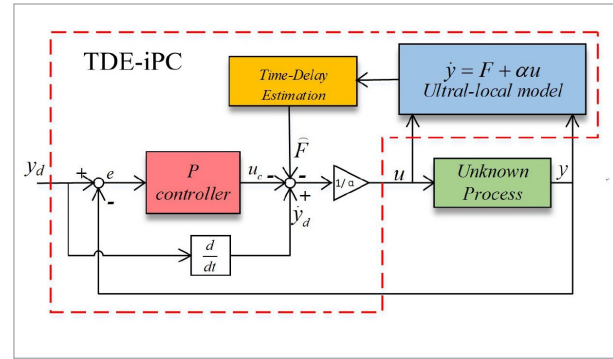
with L the selected small time delay which equals to the embedded systems' sampling time. Thus with consideration of (2), one obtains the following TDE based iP control (TDE-iPC)

$$u(t) = -\frac{\dot{y}(t - L) - \alpha u(t - L) - \dot{y}_d(t) + u_c(t)}{\alpha} \tag{5}$$

with $u_c(t) = -K_p e(t)$, and its corresponding control architecture is illustrated in Figure 1.

Figure 1
TDE-iPC control architecture

3. NFTSM-MFC

In this section, the NIB-MFC [38] is firstly presented and then a NFTSM component is added to this control algorithm in order to compensate the estimation error. The thus obtained control is called NFTSM-MFC.

3.1. NIB-MFC

The NIB-MFC can ensure the convergence rate while the convergence stability is guaranteed [38].

Define the variables

$$\begin{aligned} x_1 &= y \\ x_2 &= \dot{x}_1 \\ x_d &= y_d \end{aligned} \tag{6}$$

and denote the tracking error $y_d - y$ as

$$e_1 = x_d - x_1. \tag{7}$$

Consider the Lyapunov function as below

$$V_1(e_1) = \frac{1}{2} e_1^2. \tag{8}$$

The first derivative of (8) is

$$\dot{V}_1(e_1) = e_1 \dot{e}_1 = e_1(\dot{x}_d - x_2). \tag{9}$$

Denoting by x_2^d the costant reference of x_2, the speed tracking difference signal can be defined as

$$e_2 = x_2^d - x_2. \tag{10}$$

To guarantee the convergence of e_2 to zero, x_2^d can be chosen as

$$x_2^d = \dot{x}_d + k_1 e_1 + k_3 \int e_1 , \tag{11}$$

where $k_1 > 0$ and $k_3 > 0$ are constant parameters whose values can be determined by poles placement technique. The proportional term in (11) is employed to accelerate the convergent speed, while the proposed integral action is employed to eliminate the final steady error which is imposed from the varying and uncertain dynamics from the controlled plant [38]. The speed tracking difference signal e_2 can be rewritten as

$$e_2 = \dot{x}_d + k_1 e_1 + k_3 \int e_1 - x_2 . \tag{12}$$

The first derivatives of e_1 and e_2 are derived as below

$$\dot{e}_1 = \dot{x}_d - \dot{x}_1 = \dot{x}_d - x_2 = e_2 - k_1 e_1 - k_3 \int e_1, \tag{13}$$

$$\begin{aligned}\dot{e}_2 &= \ddot{x}_d + k_1 \dot{e}_1 + k_3 e_1 - \dot{x}_2 \\ &= \ddot{x}_d + k_1(e_2 - k_1 e_1 - k_3 \int e_1) + k_3 e_1 - \dot{x}_2 \\ &= \ddot{x}_d + k_1 e_2 - k_1^2 e_1 - k_1 k_3 \int e_1 + k_3 e_1 - \dot{x}_2 . \end{aligned} \tag{14}$$

Consider the augmented following Lyapunov functions:

$$\begin{aligned} V_1(e_1, \int e_1) &= \frac{1}{2}e_1^2 + \frac{k_3}{2}(\int e_1)^2, \\ V_2(e_1, e_2, \int e_1) &= \frac{1}{2}e_1^2 + \frac{1}{2}e_2^2 + \frac{k_3}{2}(\int e_1)^2. \end{aligned} \tag{15}$$

The first derivatives of $V_1(e_1, \int e_1)$ and $V_2(e_1, e_2, \int e_1)$ are defined as follows

$$\begin{aligned} \dot{V}_1(e_1) &= e_1 \dot{e}_1 + k_3 e_1 \int e_1 = e_1 e_2 - k_1 e_1^2 \\ \dot{V}_2(e_1, e_2, \int e_1) &= e_1 \dot{e}_1 + e_2 \dot{e}_2 + k_3 e_1 \int e_1 \\ &= e_1 e_2 - k_1 e_1^2 + e_2(\ddot{x}_d + k_1 e_2 - k_1^2 e_1 \\ &\quad - k_1 k_3 \int e_1 + k_3 e_1 - \dot{x}_2) \end{aligned} \tag{16}$$

To ensure the speed tracking which is derived on the error to zero, $\dot{V}_2(e_1, e_2)$ should be semi-negative definite. Thus, if the condition

$$e_1 e_2 + e_2(\ddot{x}_d + k_1 e_2 - k_1^2 e_1 - k_1 k_3 \int e_1 + k_3 e_1 - \dot{x}_2) = -k_2 e_2^2 \tag{17}$$

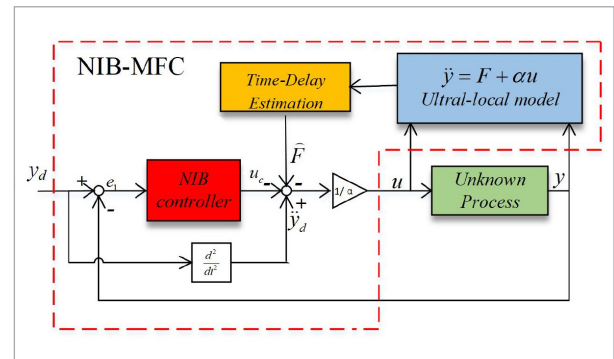is fulfilled, the speed error will tend to zero and therefore

$$\dot{x}_2 = \ddot{x}_d + (1 - k_1^2 + k_3)e_1 + (k_1 + k_2)e_2 - k_1 k_3 \int e_1 . \tag{18}$$

Based on this result, the following NIB-MFC for system (1) under its order $v = 2$ is proposed in [38] as:

$$\begin{aligned} u &= -\frac{\widehat{F} - \ddot{y}_d + u_c}{\alpha}, \\ u_c &= -(1 - k_1^2 + k_3)e_1 - (k_1 + k_2)e_2 + k_1 k_3 \int e_1 . \end{aligned} \tag{19}$$

Its NIB-MFC block diagram can be shown in the following Figure 2.

Figure 2
NIB-MFC block diagram

3.2. NFTSM-MFC

A novel MFC structure is proposed as follows, which makes possible to compensate the estimation error

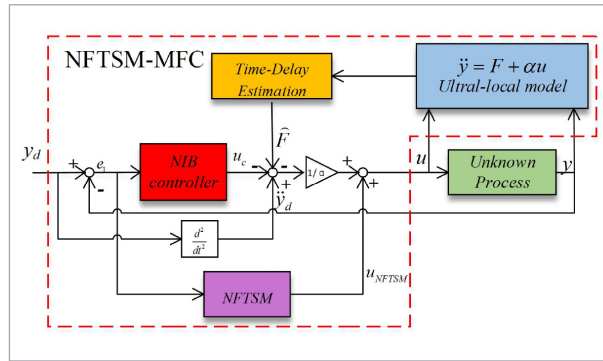$$e_{est} = F - \widehat{F} = \ddot{e} + u_c . \tag{20}$$

To this end, an additional NFTSM control is added to the NIB-MFC structure:

$$u = -\frac{\widehat{F} - \ddot{y}_d + u_c}{\alpha} + u_{NFTSM} , \tag{21}$$

here u_{NFTSM} is the additional control signal (see figure 3). Then, the closed-loop system equation is

$$\ddot{e} + u_c = \alpha u_{NFTSM} + e_{est} . \tag{22}$$

Figure 3

NFTSM-MFC block diagram

Defining the state variables

$$x_1 = e,$$
$$x_2 = \dot{e}$$

(23)

one obtains the system as follows:

$$\dot{x}_1 = x_2,$$

(24)

$$\dot{x}_2 = -u_c + \alpha u_{NFTSM} + e_{est}.$$

(25)

The estimation error e_{est} is unknown, but assuming that the system is Bounded in Input and State, and that its input derivative is bounded, then e_{est} is bounded:

$$|e_{est}| \leq E.$$

(26)

In regular SMC, its surface is usually calculated by [18]

$$s = \dot{e} + \lambda e, \ \lambda > 0.$$

(27)

However, the conventional SMC cannot ensure convergence in finite time. In order to overcome this shortcoming, terminal sliding mode (TSM) and NTSM controls are introduced [25, 43] to guarantee the convergence in finite-time. The corresponding sliding surfaces are

$$s = \dot{e} + k_1 e^{[a_1]}, k_1 > 0, 0 < a_1 < 1,$$

(28)

$$s = e + k_2 \dot{e}^{[a_2]}, k_2 > 0, 1 < a_2 < 2.$$

(29)

where s is the sliding variable and $x^{[c]} = |x|^c \ sign(x)$ with $c > 0$.

The forms of the TSM and SM sliding surface in (28) and (27) respectively for $a=1$. Because $0<a<1$, the convergence rates of TSM and NTSM are rather low than the conventional SMC. Therefore, a FTSM has been proposed to speed up the convergence [39], and its used FTSM sliding surface is defined as follows:

$$s = \dot{e} + k_1 e^{[a_1]} + k_2 e^{[a_2]}$$

(30)

where $k_1 > 0$, $k_2 > 0$, $a_1 > 0$, and $0 < a_2 < 1$. When the controlled plant is far from the equilibrium point, $k_1 e^{[a_1]}$ dominates over $k_2 e^{[a_2]}$ and equation (30) can be approached by $s = \dot{e} + k_1 e^{[a_1]} = 0$ which ensure a fast convergence. When near the equilibrium point, the term $k_2 e^{[a_2]}$ dominates over $k_1 e^{[a_1]}$ and equation (30) can be approximated by $s = \dot{e} + k_2 e^{[a_2]} = 0$ which ensures finite-time convergence. Thus, FTSM ensures a very quick convergence in the whole state space. However, the term $e^{a_2-1}\dot{e}$ in the control input may cause a singularity if $\dot{e} \neq 0$ and $e = 0$.

According to the characteristics of NTSM and FTSM, the NFTSM surface is chosen as below:

$$s = e + \sigma_1 e^{[\varphi]} + \sigma_2 \dot{e}^{[l/p]}$$

(31)

with s the sliding variable, σ_1, σ_2 the positive constants, and l and p positive odd values satisfying $1 < l/p < 2$ and $\varphi > l/p$.

To guarantee its sliding convergence, the following should satisfy

$$\dot{s} = \dot{e} + \sigma_1 \varphi |e|^{\varphi-1} \cdot \dot{e} + \sigma_2 \frac{l}{p} |\dot{e}|^{\frac{l}{p}-1} \ddot{e}$$
$$= \dot{e} + \sigma_1 \varphi |e|^{\varphi-1} \cdot \dot{e}$$
$$+ \sigma_2 \frac{l}{p} |\dot{e}|^{\frac{l}{p}-1} (-u_c + \alpha u_{NFTSM} + e_{est}).$$

(32)

The augmented control u_{NFTSM} consists of two terms [23, 39]:

$$u_{NFTSM} = u_{eq} + u_{cor}.$$

(33)

In (33), u_{eq} is called equivalent control term and obtained under $\dot{s} = 0$ as

$$u_{eq} = \frac{1}{\alpha} u_c - \frac{p}{\sigma_2 \alpha l} |\dot{e}|^{2-\frac{l}{p}} (1 + \sigma_1 \varphi |e|^{\varphi-1}).$$

(34)

u_{cor}, named as correction term, is to ensure the system reaching the sliding surface. Taking in account (26), u_{cor} can be determined as

$$u_{cor} = -\frac{1}{\alpha}(E+\lambda)\operatorname{sgn}(s), \tag{35}$$

where λ is a positive constant. Then

$$u_{NFTSM} = \frac{1}{\alpha}[u_c - (E+\lambda)\operatorname{sgn}(s)] - \frac{p}{\sigma_2 \alpha l}|\dot{e}|^{2-\frac{l}{p}}(1+\sigma_1\varphi|e|^{\varphi-1}), \tag{36}$$

and

$$u = -\frac{1}{\alpha}[\widehat{F} - \ddot{y}_d + (E+\lambda)\operatorname{sgn}(s)] - \frac{p}{\sigma_2 \alpha l}|\dot{e}|^{2-\frac{l}{p}}(1+\sigma_1\varphi|e|^{\varphi-1}). \tag{37}$$

3.3. Stability Analysis

The closed-loop system stability with NFTSM-MFC can be analyzed with Theorem 1 of [11]. The following Lyapunov function is considered

$$V = \frac{1}{2}s^2. \tag{38}$$

Taking its first derivative, one has

$$\begin{aligned}
\dot{V} = s\dot{s} &= (e+\sigma_1 e^{[\varphi]} + \sigma_2 \dot{e}^{[l/p]})[\dot{e}+\sigma_1\varphi|e|^{\varphi-1} \\
&\quad + \sigma_2\frac{l}{p}|\dot{e}|^{\frac{l}{p}-1}(e_{est}-(E+\lambda)\operatorname{sgn}(s) \\
&\quad - \frac{p}{\sigma_2 l}|\dot{e}|^{2-\frac{l}{p}}(1+\sigma_1\varphi|e|^{\varphi-2}))] \\
&= (e+\sigma_1 e^{[\varphi]} + \sigma_2 \dot{e}^{[l/p]}) \\
&\quad [\sigma_2\frac{l}{p}|\dot{e}|^{\frac{l}{p}-1}(e_{est}-(E+\lambda)\operatorname{sgn}(s))] \\
&= \sigma_2\frac{l}{p}|\dot{e}|^{\frac{l}{p}-1}(e_{est}s-(E+\lambda)\operatorname{sgn}(s)s) \\
&\leq -\sigma_2\frac{l}{p}|\dot{e}|^{\frac{l}{p}-1}\lambda|s|.
\end{aligned} \tag{39}$$

Since l, p and σ_2 are positive, then:

1 for $\dot{e} \neq 0$, one has $\dot{V} < 0$ and $s = 0$ obtained in finite time;

2 for $\dot{e} = 0$, by substituting (36) into (22), one obtains

$$\ddot{e} = -(E+\lambda)\operatorname{sgn}(s) + e_{est}. \tag{40}$$

For $s > 0$ one has $\ddot{e} < -\lambda$ and for $s < 0$ one has $\ddot{e} > \lambda$, which means that $\dot{e}$ is not an attractor. This also means that for a small $\xi > 0$ there exists neighborhood $|\dot{e}| \leq \xi$ of $\dot{e} = 0$, such that $\ddot{e} < -\lambda$ for $s > 0$ and $\ddot{e} > \lambda$ for $s < 0$. Thus, according to [11], the finite-time sliding surface crossing for the system states, $\dot{e} = \xi$ to $\dot{e} = -\xi$ for $s > 0$ and from $\dot{e} = -\xi$ to $\dot{e} = \xi$ for $s < 0$, can be guaranteed. While in others under $|\dot{e}| > \xi$, the sliding surface can be obtained in finite time, since $\ddot{e} < -\lambda$ for $s > 0$, and $\ddot{e} > \lambda$ for $s < 0$. Thus, the referred s=0 could be attained in finite time from anywhere. Meanwhile, the control algorithm (34) is always nonsingular with $1 < l/p < 2$.

Therefore NFTSM-MFC ensures system stability and convergence in finite time from any initial different states without any singularity.

4. Glucose-Insulin Dynamic Model

The proposed controller is implemented and evaluated for a type 1 diabetes long-term glucose-insulin dynamic model [15, 16, 24, 28, 34].

This proposed model makes possible to overcome the following two common drawbacks by comparing to other mathematical system models. The first drawback is that the existing models can only predict glucose level for a rather short time, only capable to fit clinical data for a few hours [34], or with up-limit of $20h$ [15, 28]. The second common drawback is that the model is not capable to take functional insulin therapy into account [16]. While this proposed long-term model, it can predict closely glycemia behavior to few days with validation with diabetic patients clinical data taken form Rennes and Nantes University-Hospital Centers [24].

The proposed long-term model in [24] consists three parts which describe the glucose, insulin and digestion dynamics respectively. The proposed glucose-insulin model is denoted as follows [24]:

$$
\begin{bmatrix} \dot{G} \\ \dot{I} \\ \ddot{I} \\ \dot{D} \\ \ddot{D} \end{bmatrix} = \begin{bmatrix} 0 & -k_{si} & 0 & 1 & 0 \\ 0 & 0 & 1 & 0 & 0 \\ 0 & -\dfrac{1}{T_u^2} & -\dfrac{2}{T_u} & 0 & 0 \\ 0 & 0 & 0 & 0 & 1 \\ 0 & 0 & 0 & -\dfrac{1}{T_r^2} & -\dfrac{2}{T_r} \end{bmatrix} \cdot \begin{bmatrix} G \\ I \\ \dot{I} \\ D \\ \dot{D} \end{bmatrix} + \begin{bmatrix} 0 & 0 \\ 0 & 0 \\ \dfrac{k_u}{V_i \cdot T_u^2} & 0 \\ 0 & 0 \\ 0 & \dfrac{k_r}{V_B \cdot T_r^2} \end{bmatrix} \begin{bmatrix} u \\ r \end{bmatrix} + \begin{bmatrix} k_l - \dfrac{128}{M} \\ 0 \\ 0 \\ 0 \\ 0 \end{bmatrix},
\tag{41}
$$

where $u(t)$ is input insulin injection rate (U/min), $G(t)$ is first element of the state representing glucose level (mg/dL), $I(t)$ is the second element of the state representing insulin level (U/dL), $D(t)$ is glucose appearance rate in the result of the carbohydrate digestion ($mg/(dL*min)$), $r(t)$ is the carbohydrate in meal (mg). The parameter values for three patients (IF2, IF3, BE) are given in Appendix A. The parameters for each patient are identified by fitting the corresponding CGM data thus several virtual patients can be established as the control objects. In addition, measurement noise is added to simulate the actual situation.

The control objectives can be divided into two by accoring to different stages of virtual patients, called normal stage and postprandial stage. At the normal stage, the glycemia need to be maintained in the range of l [70, 120]mg/dL. At the postprandial stage, the glycemia need to be kept under [120, 170]mg/dL in the 1st 60 minutes, and need not to exceed 140 mg/dL in the 2nd 60 minutes then returning to normal levels within 180 minutes. And the hypoglycemia should be prevented as glycemia is under 70 mg/dL, where the life safety of patients will be threatened.

5. Glycemia Regulation Using NFTSM-MFC

In this section, the NFTSM-MFC is applied to the glucose-insulin dynamics model (41) and its performances are compared with those of TDE-iPC and NIB-MFC for the three virtual patients IF2, IF3 and BE. In TDE-iPC, α is set to 2000000 and kept in con-

stant value, and K_p is set per patient to 1.2 (IF2), 0.45 (IF3), and 0.6 (BE). In NIB-MFC α is set to 1800. For IF3 the following values of parameters are chosen: k_1=0.0005, k_2=0.0001, k_3=0.4. The corresponding parameters values for BE are k_1=0.04, k_2=0.0005, k_3=0.8, and for IF2 these values are k_1=0.05, k_2=0.0001, k_3=0.5. The values of parameters in NFTSM-MFC are chosen as E=0.1, λ=0.5, p=17, l=19, δ_1=0.1, δ_2=0.1, ϕ=1.3.

For the patient IF3, the considered controllers are compared for the following three cases: $G(0) = 160 mg/dL$, $G(0) = 40 mg/dL$, and taking a meal represented by the carbohydrates intake rate $r = 100 \exp(-5t)g$ at $t = 1h$. The numerical results are illustrated in Fig. 4. It shows that in the considered cases the three controllers succeed to force glucose to the desired value. The NIB-MFC and NFTSM-MFC ensure a quite similar convergence, faster than the convergence using TDE-iPC. Concerning the overshoot and steady-state error, the NFTSM-MFC shows superiority than the NIB-MFC and the NFTSM-MFC without NIB.

In the next simulation, several regular meals are taking by the virtual patient IF3 to test the performance in daily situation. The corresponding results as illustrated in Figure 5. Furthermore, situation of large amount of meal intake for the virtual patient BE is simulated to evaluate hypoglycemic ability. The obtained results are shown in Figure 6. Finally, for the virtual patient IF2, the considered controllers are compared for the situation in snack time, with small amounts and frequent carbohydrate intake. The corresponding results are shown in Figure 7. The summaries of simulation statistics are given in Appendix B.

Figure 4

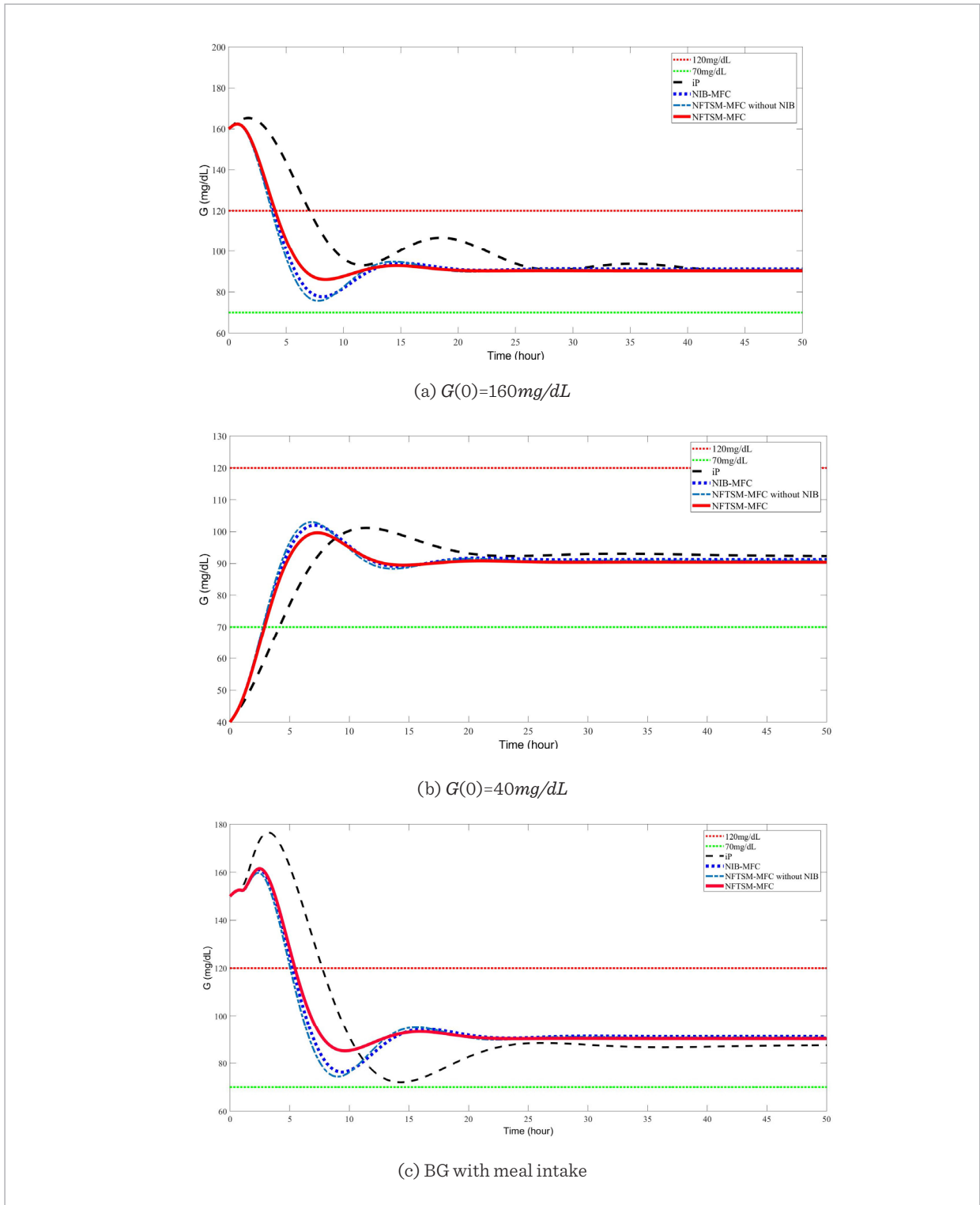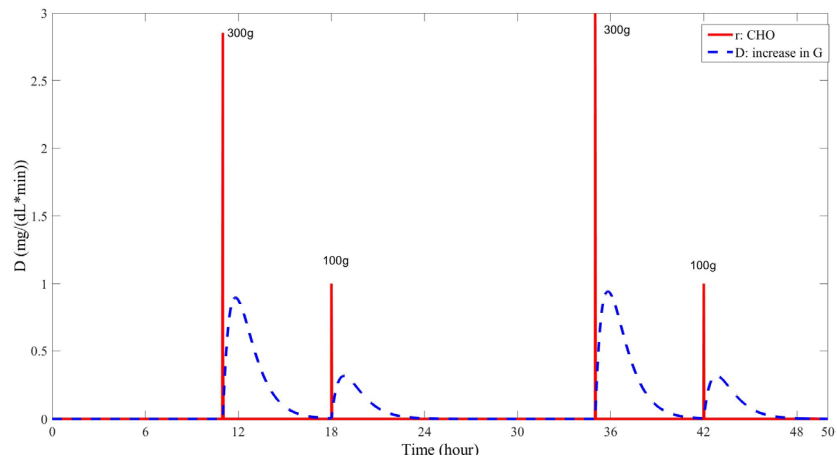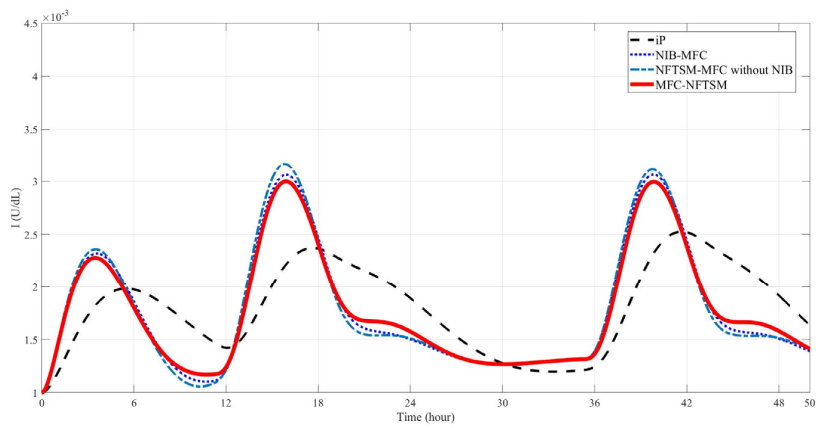IF3 virtual patient responses for TDE-iPC, NIB-MFC, NFTSM-MFC without NIB and NFTSM-MFC

(a) $G(0)=160mg/dL$

(b) $G(0)=40mg/dL$
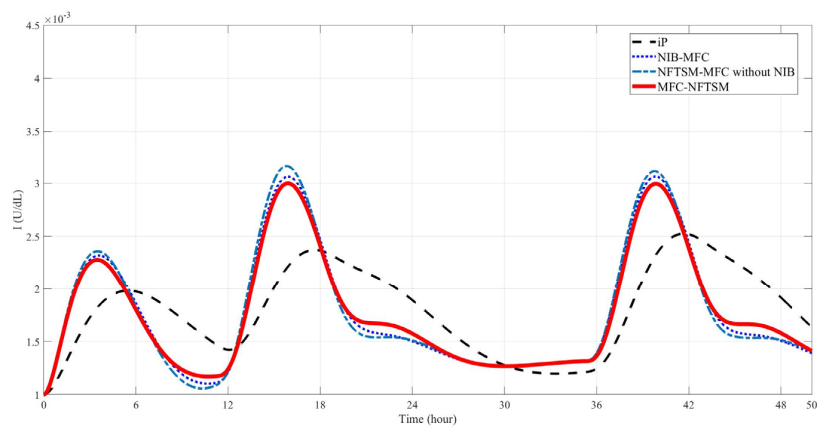
(c) BG with meal intake

Figure 5

IF3 virtual patient responses for TDE-iPC, NIB-MFC, NFTSM-MFC without NIB and NFTSM-MFC

(a) BG behavior

(b) Meals and corresponding glucose rate of appearance

(c) Insulinemia
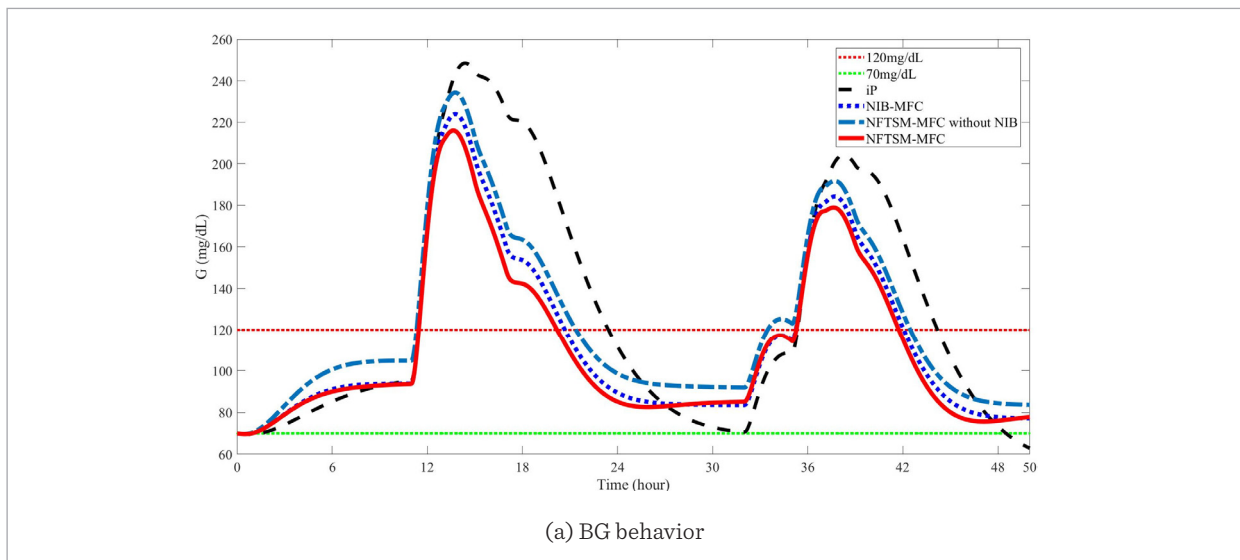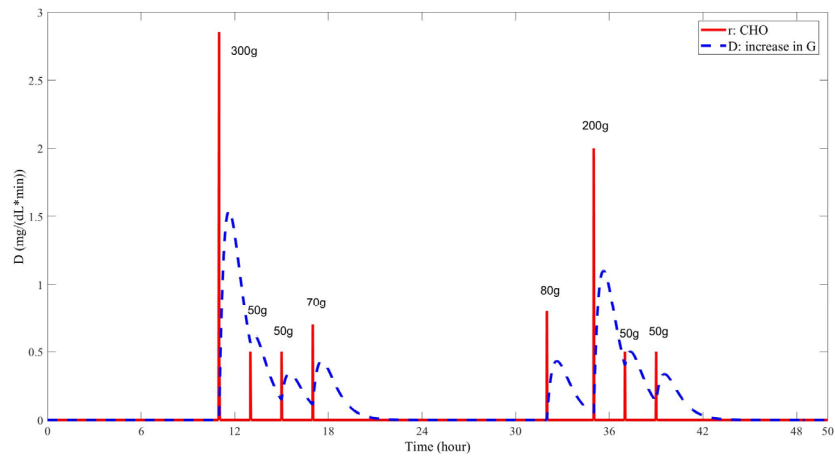
(d) Insulin infusion rate
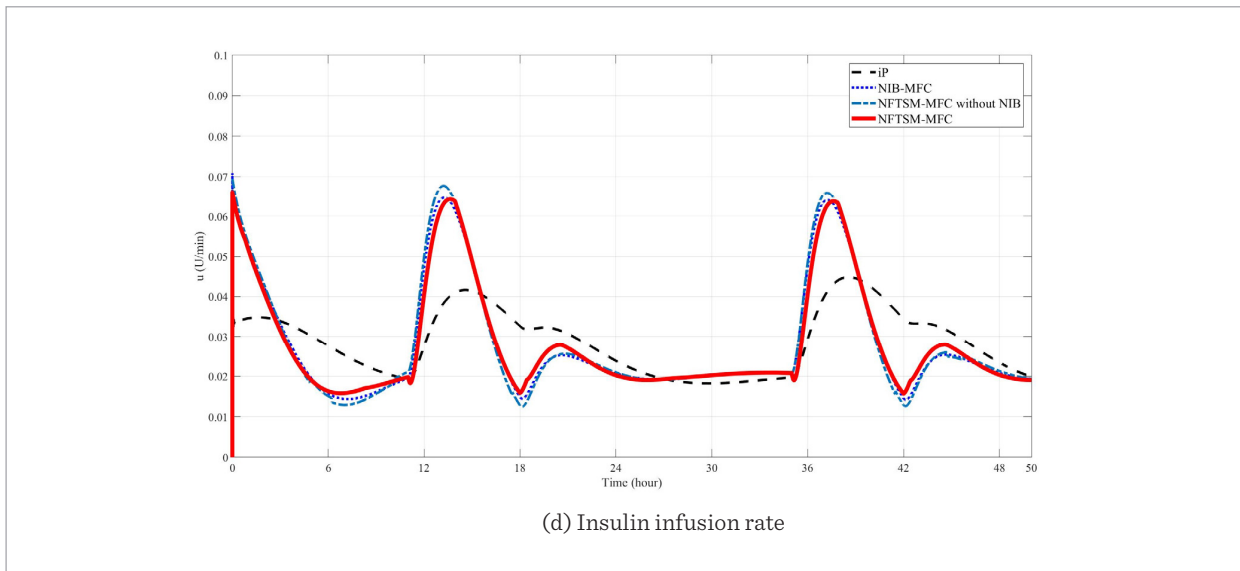
The simulation results presented in Figures 5, 6 and 7 show the higher performances of NIB-MFC compared to TDE-iPC. The hyperglycemia is substantially reduced using NIB-MFC, especially when postprandial phase is detected. In particular figure 7(a) shows that overdose of insulin and possible hypoglycemia could be more easily prevented by NIB-MFC than by TDE-iPC. The global BG mean value is upgraded and overshoots are decreased.

Due to compensation of the estimation error in TDE, the NFTSM-MFC is more efficient than NIB-MFC. The NFTSM-MFC makes possible to achieve smaller max value of G, bigger min value of G, mean of G closer to desired value, smaller overshoots, shorter hyperglycemia and hypoglycemia phases and smaller mean of $u(t)$.

Figure 6

BE virtual patient responses for TDE-iPC, NIB-MFC, NFTSM-MFC without NIB and NFTSM-MFC

(a) BG behavior

(b) Meals and corresponding glucose rate of appearance

(c) Insulinemia

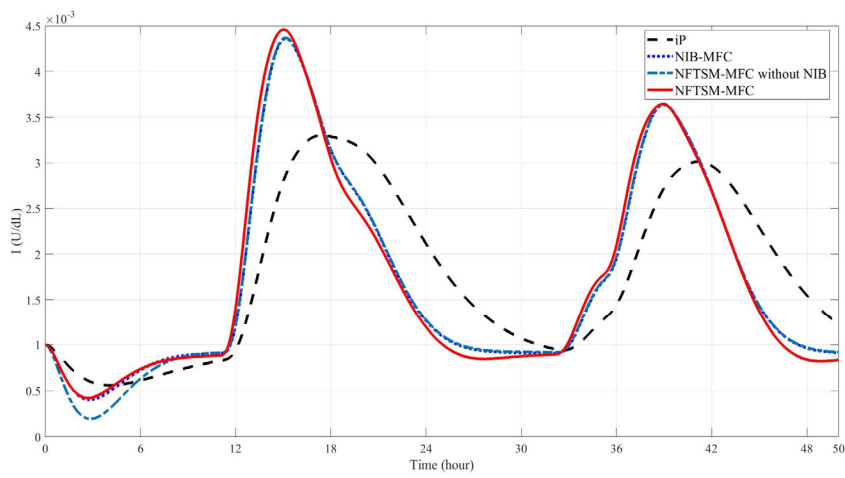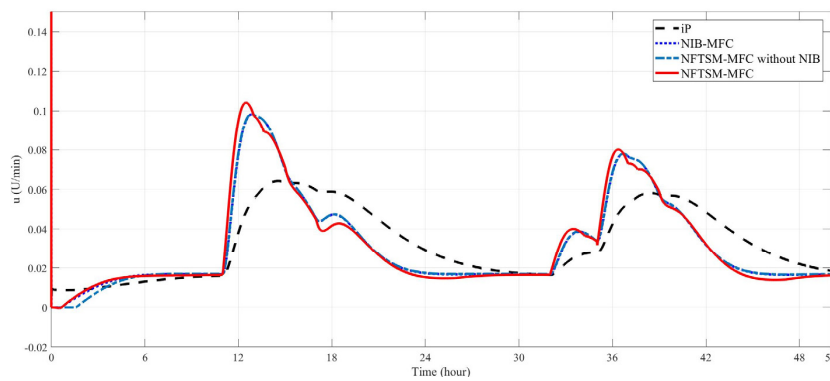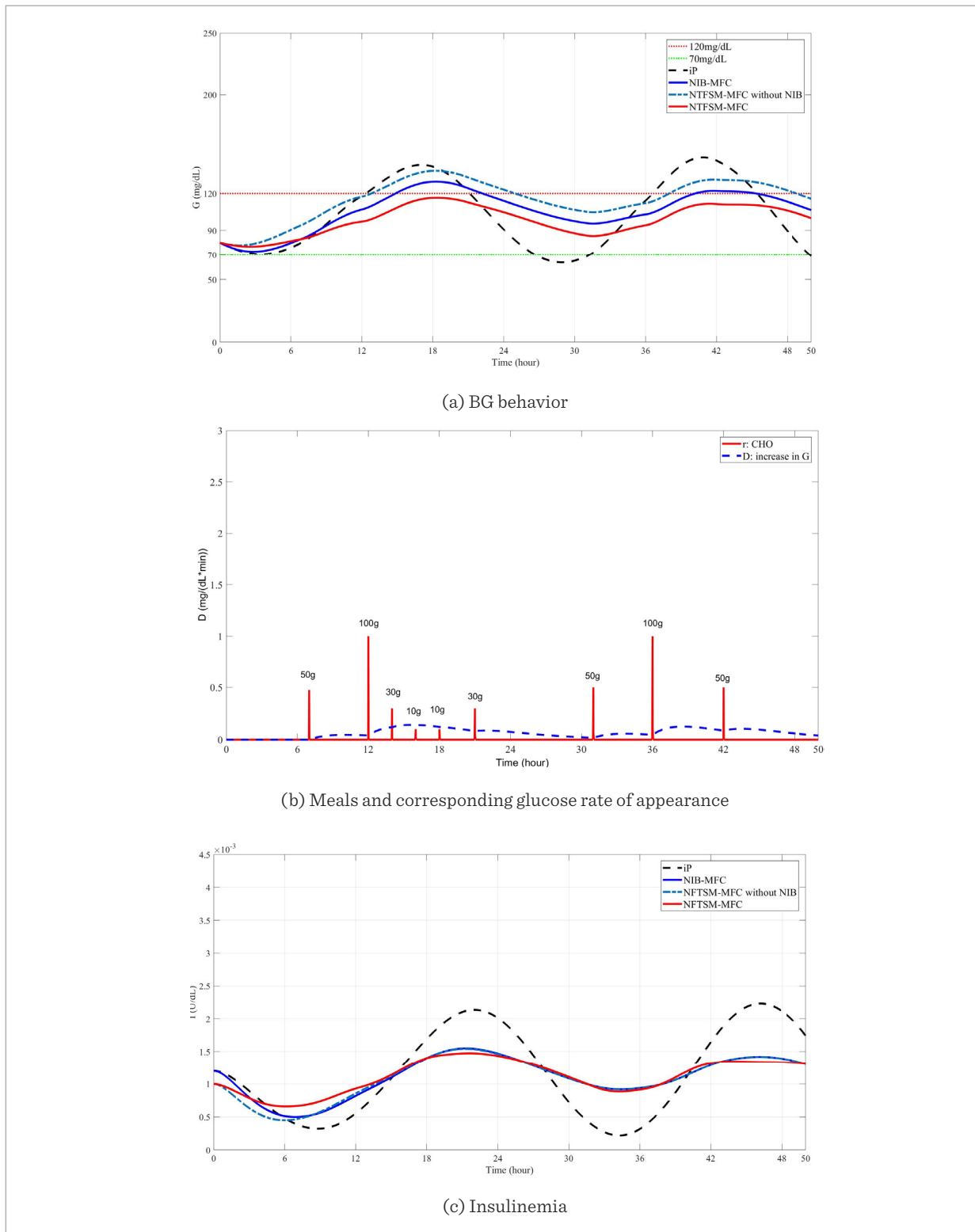(d) Insulin infusion rate

Figure 7

IF2 virtual patient responses for TDE-iPC, NIB-MFC, NFTSM-MFC without NIB and NFTSM-MFC

(a) BG behavior

(b) Meals and corresponding glucose rate of appearance
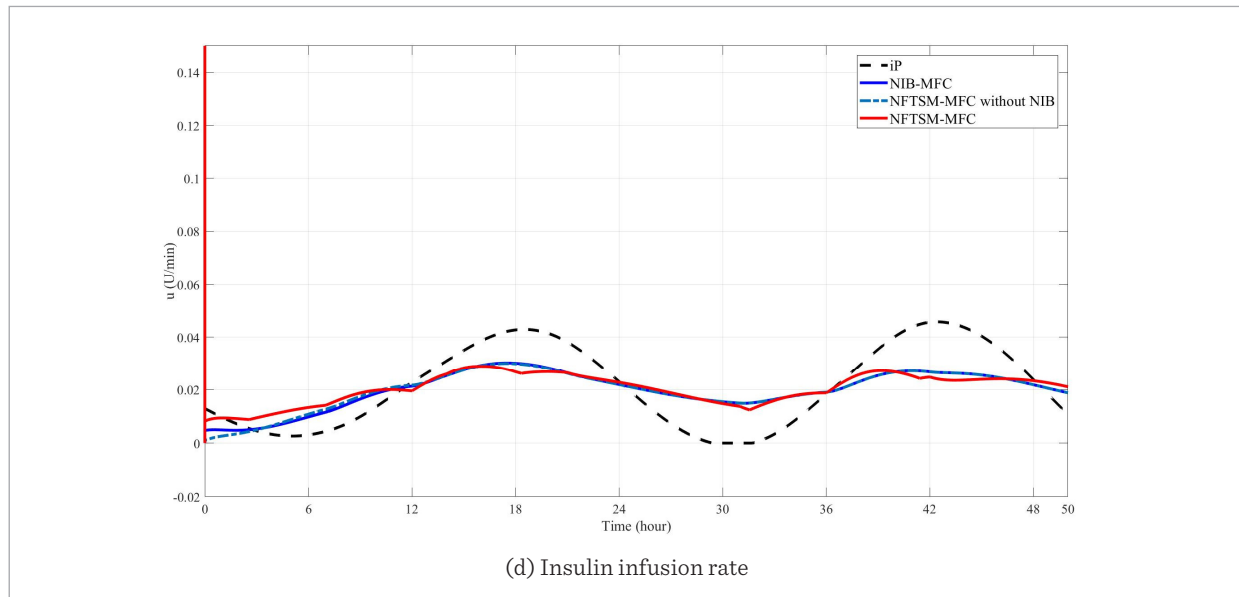
(c) Insulinemia

(d) Insulin infusion rate

6. Conclusion

In conclusion, a NFTSM-MFC is proposed and its application to glucose regulation systems is considered. The new control structure is obtained by adding a NFTSM component to the well-known NIB-MFC in order to compensate the estimation error of the TDE module of NIB-MFC. The corresponding system stability under the new controller is analyzed and the application of NFTSM-MFC for glycemia regulation is considered. The numerical simulations show that NFTSM-MFC can stabilize glycemia level more rapidly and with small error than the NIB-MFC and intelligent proportional control for a glucose-insulin dynamic model of a T1DM patient for long-term simulation.

References

1. Abouaïssa, H., Fliess, M., Join, C. On Ramp Metering: Towards a Better Understanding of ALINEA via Model-Free Control. International Journal of Control, 2017, 90(5), 1018-1026. https://doi.org/10.1080/00207179.2016.1193223

2. Abouaïssa, H., Hasan, O. A., Join, C., Fliess, M., Defer, D. Energy Saving for Building Heating via a Simple and Efficient Model-Free Control Design: First Steps with Computer Simulations. Proceedings of 21st International Conference on System Theory, Control and Computing, 2017, 747-752. https://doi.org/10.1109/ICSTCC.2017.8107126

3. Al Younes, Y., Drak, A., Noura, H., Rabhi, A., El Hajjaji, A. Model-Free Control of a Quadrotor Vehicle. Proceeding of 2014 IEEE Conference on Unmanned Aircraft Systems (ICUAS), 1126-1131. https://doi.org/10.1109/ICUAS.2014.6842366

4. Al Younes, Y., Drak, A., Noura, H., Rabhi, A., El Hajjaji, A. Robust Model-Free Control Applied to a Quadrotor UAV. Journal of Intelligent and Robotic Systems, 2016, 84(1-4), 37-52. https://doi.org/10.1007/s10846-016-0351-2

5. Bhattacharjee, A., Sutradhar, A. Data Driven Nonparametric Identification and Model Based Control of Glucose-Insulin Process in Type 1 Diabetics. Journal of Process Control, 2016, 41, 14-25. https://doi.org/10.1016/j.jprocont.2016.02.003

6. Campi, M.C., Lecchini, A., Savaresi, S. Virtual Reference Feedback Tuning: A Direct Method for the Design of

Feedback Controllers. Automatica, 2002, 38(8), 1337-1346. https://doi.org/10.1016/S0005-1098(02)00032-8

7. Cobelli, C., Renard, E., Kovatchev, B. Artificial Pancreas: Past, Present, Future. Diabetes Care, 2011, 60(11), 2672-2682. https://doi.org/10.2337/db11-0654

8. Craven, S., Whelan, J., Glennon, B. Glucose Concentration Control of a Fed-Batch Mammalian Cell Bioprocess Using a Nonlinear Model Predictive Controller. Journal of Process Control, 2014, 24(4), 344-357. https://doi.org/10.1016/j.jprocont.2014.02.007

9. Del Favero, S., Bruttomesso, D., Di Palma, F., Lanzola, G., Visentin, R., Filippi, A., Scotton, R., Toffanin, C., Messori, M., Scarpellini, S. First Use of Model Predictive Control in Outpatient Wearable Artificial Pancreas. Diabetes Care, 2014, 37(5), 1212-1215. https://doi.org/10.2337/dc13-1631

10. Dua, P., Doyle, F.J., Pistikopoulos, E. N. Model-Based Blood Glucose Control for Type 1 Diabetes via Parametric Programming. IEEE Transactions on Biomedical Engineering, 2006, 53(8), 1478-1491. https://doi.org/10.1109/TBME.2006.878075

11. Feng, Y., Yu, X., Man, Z. Non-Singular Terminal Sliding Mode Control of Rigid Manipulators. Automatica, 2002, 38(12), 2159-2167. https://doi.org/10.1016/S0005-1098(02)00147-4

12. Fliess, M., Join, C. Model-Free Control and Intelligent PID Controllers: Towards a Possible Trivialization of Nonlinear Control? IFAC Proceedings, 2009, 42(10), 1531-1550. https://doi.org/10.3182/20090706-3-FR-2004.00256

13. Fliess, M., Join, C. Model-Free Control. International Journal of Control, 2013, 86(12), 2228-2252. https://doi.org/10.1080/00207179.2013.810345

14. Fliess, M., Join, C., Sira-Ramirez, H. Non-Linear Estimation Is Easy. International Journal of Modelling, Identification and Control, 2008, 4(1), 12-27. https://doi.org/10.1504/IJMIC.2008.020996

15. Haidar, A., Wilinska, M. E., Graveston, J.A., Hovorka, R. Stochastic Virtual Population of Subjects with Type 1 Diabetes for the Assessment of Closed-Loop Glucose Controllers. IEEE Transactions on Biomedical Engineering, 2013, 60(12), 3524-3533. https://doi.org/10.1109/TBME.2013.2272736

16. Hanaire, H., Lassmann-Vague, V., Jeandidier, N., Renard, E., Tubiana-Rufi, N., Vambergue, A., Raccah, D., Pinget, M., Guerci, B. Treatment of Diabetes Mellitus Using an External Insulin Pump: The State of the Art. Diabetes & Metabolism, 2008, 34(4), 401-423. https://doi.org/10.1016/S1262-3636(08)73972-7

17. Hou, Z., Liu, S., Tian, T. Lazy-Learning-Based Data-Driven Model-Free Adaptive Predictive Control for a Class of Discrete-Time Nonlinear Systems. IEEE Transactions on Neural Networks and Learning Systems, 2017, 28(8), 1914-1928. https://doi.org/10.1109/TNNLS.2016.2561702

18. Islam, S., Liu, X.P. Robust Sliding Mode Control for Robot Manipulators. IEEE Transactions on Industrial Electronics, 2011, 58(6), 2444-2453. https://doi.org/10.1109/TIE.2010.2062472

19. Jin, Z., Chen, J., Sheng, Y., Liu, X. Neural Network Based Adaptive Fuzzy PID-Type Sliding Mode Attitude Control for a Reentry Vehicle. International Journal of Control, Automation and Systems, 2017, 15(1), 404-415. https://doi.org/10.1007/s12555-015-0181-1

20. Kaveh, P., Shtessel, Y.B. Blood Glucose Regulation Using Higher Order Sliding Mode Control. International Journal of Robust and Nonlinear Control, 2008, 18(4-5), 557-569. https://doi.org/10.1002/rnc.1223

21. Kim, M., Kuc, T. Y., Kim, H., Lee, J. Adaptive Iterative Learning Controller with Input Learning Technique for a Class of Uncertain MIMO Nonlinear Systems. International Journal of Control, Automation and Systems, 2017, 15(1), 315-328. https://doi.org/10.1007/s12555-016-0049-z

22. Li, C., Yi, J., Wang, T. Encoding Prior Knowledge into Data Driven Design of Interval Type-2 Fuzzy Logic Systems. International Journal of Innovative Computing, Information and Control, 2011, 7(3), 1133-1144.

23. Li, H., Dou, L., Su, Z. Adaptive Nonsingular Fast Terminal Sliding Mode Control for Electromechanical Actuator. International Journal of Systems Science, 2013, 44(3), 401-415. https://doi.org/10.1080/00207721.2011.601348

24. Magdelaine, N., Chaillous, L., Guilhem, I., Poirier, J.Y., Krempf, M., Moog, C.H., Le Carpentier, E. A Long-Term Model of the Glucose-Insulin Dynamics of Type 1 Diabetes. IEEE Transactions on Biomedical Engineering, 2015, 62(6), 1546-1552. https://doi.org/10.1109/TBME.2015.2394239

25. Man, Z., O'day, M., Yu, X. A Robust Adaptive Terminal Sliding Mode Control for Rigid Robotic Manipulators. Journal of Intelligent Robotic Systems, 1999, 24(1), 23-41.

26. Marchetti, G., Barolo, M., Jovanovic, L., Zisser, H., Seborg, D.E. An Improved PID Switching Control Strategy for Type 1 Diabetes. IEEE Transactions on Biomedical Engineering, 2008, 55(3), 857-865. https://doi.org/10.1109/TBME.2008.915665

27. Mohammad Ridha, T., Moog, C.H., Delaleau, E., Fliess, M., Join, C. A Variable Reference Trajectory for Mod-

el-Free Glycemia Regulation. Proceedings of 2015 SIAM Conference on Control and its Applications, 2015, 60-67. https://doi.org/10.1137/1.9781611974072.9

28. Mohammad Ridha, T., Ait-Ahmed, M., Chaillous, L., Krempf, M., Guilhem, I., Poirier, J. Y., Moog, C. H. Model Free iPID Control for Glycemia Regulation of Type-1 Diabetes. IEEE Transactions on Biomedical Engineering, 2018, 65(1), 199-206. https://doi.org/10.1109/TBME.2017.2698036

29. Ottavian, M., Barolo, M., Zisser, H., Dassau, E., Seborg, D. E. Improved Blood Glucose Control for Critically Ill Subjects. Journal of Process Control, 2011, 21(3), 331-342. https://doi.org/10.1016/j.jprocont.2010.07.003

30. Percival, M., Wang, Y., Grosman, B., Dassau, E., Zisser, H., Jovanovič, L., Doyle III, F. Development of A Multi-Parametric Model Predictive Control Algorithm for Insulin Delivery in Type 1 Diabetes Mellitus Using Clinical Parameters. Journal of Process Control, 2011, 21(3), 391-404. https://doi.org/10.1016/j.jprocont.2010.10.003

31. Plank, J., Blaha, J., Cordingley, J., Wilinska, M.E., Chassin, L. J., Morgan, C., Squire, S., Haluzik, M., Kremen, J., Svacina, S. Multicentric, Randomized, Controlled Trial to Evaluate Blood Glucose Control by the Model Predictive Control Algorithm versus Routine Glucose Management Protocols in Intensive Care Unit Patients. Diabetes Care, 2006, 29(2), 271-276. https://doi.org/10.2337/diacare.29.02.06.dc05-1689

32. Ridha, T. M. M., Kadhum, M. Q., Mahdi, S. M. Back Stepping-Based-PID-Controller Designed for an Artificial Pancreas Model. Al-Khwarizmi Engineering Journal, 2011, 7(4), 54-60.

33. Rojas, J., Vilanova, R. Data-Driven Based IMC Control. International Journal of Innovative Computing, Information and Control, 2012, 8(3), 1557-1574.

34. Stahl, F., Johansson, R. Short-Term Diabetes Blood Glucose Prediction Based on Blood Glucose Measurements. Proceedings of 30th International Conference of the Engineering in Medicine and Biology Society, 2008, 291-294. https://doi.org/10.1109/IEMBS.2008.4649147

35. Tian, Y., Wang, H., Vasseur, C. Adaptive Optimal Trajectory Tracking Control of Nonlinear Affine in Control System with Unknown Internal Dynamics. Proceedings of 33rd Chinese Control Conference, 2014, 2234-2239. https://doi.org/10.1109/ChiCC.2014.6896979

36. Wang, H., Tian, Y., Christov, N. Piecewise-Continuous Observers for Linear Systems with Sampled and Delayed Output. International Journal of Systems Science, 2016, 47(8), 1804-1815. https://doi.org/10.1080/00207721.2014.953798

37. Wang, H., Vasseur, C., Christov, N., Koncar, V. Vision Servoing of Robot Systems Using Piecewise Continuous Controllers and Observers. Mechanical Systems and Signal Processing, 2012, 33, 132-141. https://doi.org/10.1016/j.ymssp.2012.06.022

38. Wu, Q., Wang, H., Tian, Y. Model Free Control Based Nonlinear Integral-Backstepping Control for Blood Glucose Regulation. Proceedings of 6th IEEE Data Driven Control and Learning Systems Conference, 2017 May 26, 94-99. https://doi.org/10.1109/DDCLS.2017.8068051

39. Yang, L., Yang, J. Nonsingular Fast Terminal Sliding-Mode Control for Nonlinear Dynamical Systems. International Journal of Robust and Nonlinear Control, 2011, 21(16), 1865-1879. https://doi.org/10.1002/rnc.1666

40. Yin, S., Ding, S. X., Abandan Sari, A. H., Hao, H. Data-Driven Monitoring for Stochastic Systems and Its Application on Batch Process. International Journal of Systems Science, 2013, 44(7), 1366-1376. https://doi.org/10.1080/00207721.2012.659708

41. Yin, S., Luo, H., Ding, S. X. Real-Time Implementation of Fault-Tolerant Control Systems with Performance Optimization. IEEE Transactions on Industrial Electronics, 2014, 61(5), 2402-2411. https://doi.org/10.1109/TIE.2013.2273477

42. Youcef-Toumi, K., Fuhlbrigge, T. A. Application of Decentralized Time-Delay Controller to Robot Manipulators. Proceedings of 1989 IEEE Conference on Robotics and Automation, 1989 May 14, 1786-1791.

43. Yu, S., Yu, X., Shirinzadeh, B., Man, Z. Continuous Finite-Time Control for Robotic Manipulators with Terminal Sliding Mode. Automatica, 2005, 41(11), 1957-1964. https://doi.org/10.1016/j.automatica.2005.07.001

44. Zhang, X., Wang, H., Tian, Y., Peyrodie, L., Wang, X. Model-Free Based Neural Network Control with Time-Delay Estimation for Lower Extremity Exoskeleton. Neurocomputing, 2018, 272, 178-188. https://doi.org/10.1016/j.neucom.2017.06.055

45. Zhao, B., Li, Y. Model-Free Adaptive Dynamic Programming Based Near-Optimal Decentralized Tracking Control of Reconfigurable Manipulators. International Journal of Control, Automation and Systems, 2018, 16(2), 478-490. https://doi.org/10.1007/s12555-016-0711-5

46. Zhao, D.J., Yang, D.G. Model-Free Control of Quad-Rotor Vehicle via Finite-Time Convergent Extended State Observer. International Journal of Control, Automation and Systems, 2016, 14(1), 242-254. https://doi.org/10.1007/s12555-013-0355-7

Appendix A

Model parameters and its values for IF2, IF3, BE

Parameter	Definition	Units	IF2	IF3	BE
M	Body weight	kg	72	94	73.5
K_{si}	Gain for effect of insulin	$\dfrac{mg}{U*min}$	197	274	186
T_u	Insulin dynamics time constant	min	122	88	59
V_i	Equivalent volume for insulin dispersion	dL	10	15	10
K_u/V_i	Constant	min/dL	180	235	183.75
T_r	Time constant for individual difference	min	183	49	38
V_B	Equivalent volume for blood	dL	0.11	0.1248	0.13
T_r/V_B	Constant	min/dL	46.8	61.1	47.775
$K_l - 128/M$	Endogenous glucose production	$\dfrac{mg}{dL*min}$	1.94	1.72	1.91

Appendix B

Simulation statistics

Parameter	IF3			BE			IF2		
	TDE-iPC	NIB-MFC	NFTSM-MFC	TDE-iPC	NIB-MFC	NFTSM-MFC	TDE-iPC	NIB-MFC	NFTSM-MFC
Max glucose level (mg/dL)	186.8	182	179.1	248.5	224	216.1	149.2	129.6	127.7
Min glucose level (mg/dL)	70.06	79.62	75.47	62.89	69.66	69.66	63.74	72.64	72.25
Hyperglycemia period (G>200) (h)	/	/	/	7	2.4	2.1	/	/	/
Hypoglycemia period (G<70) (h)	/	/	/	2	1.4	14	4.7	/	/
Mean glucose level (mg/dL)	118.2	110.9	108.1	128.7	114.6	111.2	104.2	106.3	105.2
Standard Deviation of glucose level (mg/dL)	35.72	29.55	29.28	57.16	41.03	38.68	27.96	16.06	15.88
Mean insulin level (U/h)	1.7265	1.6900	1.3068	1.9410	1.8912	1.6872	1.2954	1.1976	1.1976